공학석사학위논문

디젤엔진의 연소음 저감을 위한 열발생률 설계인자에 관한 연구

Design Factor of Heat Release Rate Shaping for Combustion Noise Reduction in a Diesel Engine

2015 년 8 월

서울대학교 대학원

기계항공공학부

이 성 문

디젤엔진의 연소음 저감을 위한 열발생률 설계인자에 관한 연구

Design Factor of Heat Release Rate Shaping for Combustion Noise Reduction in a Diesel Engine

지도교수 민 경 덕

이 논문을 공학석사 학위논문으로 제출함

2015 년 8 월

서울대학교 대학원

기계항공공학부

이 성 문

이성문의 공학석사 학위논문을 인준함

2015 년 6 월

위 원 장 _____고___상___근____(인)

부위원장 _____민___경___덕____(인)

위　　원 _____송___한___호____(인)

Abstract

Design Factor of Heat Release Rate Shaping for Combustion Noise Reduction in a Diesel Engine

Sungmoon Lee

Department of Mechanical and Aerospace Engineering

The Graduate School

Seoul National University

Advancement of diesel engine development has been heading for the cleanness, high performance and comfortability. In comparison of spark-ignition engine, it has several drawbacks due to its combustion characteristic with high compression ratio. Noise and vibration are widely known as a major representative issue of diesel engine in an aspect to passenger's drivability.

This study simulates the shape of heat release rate by manipulating measured burning rate to figure out the effect of its shape to combustion noise level. Conventional approach for noise reduction is the way of changing combustion parameters with the noise measurement to optimize them. New method reaches to the goal on the contrary to the previous approach. It is focused on the shape of heat release rate and its effect to the combustion noise level. Design factors for shaping optimal heat release rate were derived first. Combustion parameters were chosen to achieve the suggested shape in order.

Combustion Noise Index (CNI) from simulated in-cylinder pressure was used as an indicator of direct combustion noise. Consequently, design factors affecting to CNI were combustion phase, peak and width of heat release rate. Lower peak of heat release rate, wider heat release rate and retarded combustion phase have an effect to decrease in CNI.

Combustion parameters were selected in respect to the design factors and experimentally verified in sequence so as to confirm the feasibility. Exhaust gas emission and bmep were also considered. Fuel injection timing, pressure, EGR ratio, swirl and pilot quantity were changed and inspected to figure the response of CNI to the shape of heat release rate.

In consequence, CNI decreased from the base condition by 3.6 dB without any increase in exhaust gas emissions and los of bmep by using these combustion parameters. The experiment was conducted from the base condition by changing parameters. Its responses to three design factors, which are the combustion phase, pHRR and width of heat release rate were considered simultaneously. While the CNI reaches to the lower level with reasonable exhaust gas emissions and bmep, entire procedure was divided into three steps. The first step is the retard of main injection timing and reduced swirl. Second, injection pressure was reduced. Lastly, EGR ratio decreased.

Keywords: Heat Release Rate, Heat Release Rate Shaping, Combustion Noise Index (CNI), Combustion Noise, Diesel Engine, Noise Reduction

Student Number: 2013-23081

Contents

List of Tables

List of Figures

Acronym

aTDC	After Top Dead Center
bTDC	Before Top Dead Center
CAD	Crank Angle Degree
ECU	Engine Control Unit
HRR	Heat Release Rate
CNI	Combustion Noise Index
pHRR	Peak of Heat Release Rate
PM	Particulate Matter
NO_x	Nitrogen Oxides
bmep	Brake Mean Effective Pressure
imep	Indicated Mean Effective Pressure
EGR	Exhaust Gas Recirculation
MIT	Main Injection Timing
THC	Total Hydrocarbon
CA50	50% of Mass Fraction Burned Crank Angle
AR	Aspect Ratio
RPM	Rotate Per Minute
IC	Intercooler
SOI	Start of Injection
EOI	End of Injection
CN	Cetane Number

Chapter 1. Introduction

1.1 Background and Motivation

1.1.1 Noise and Vibration Issue of a Diesel Engine

Further internal combustion engine development has been achieved in the direction of cleanness, high performance and comfortability from light to heavy duty vehicles. Cleanness includes not only harmful gases, such as nitrogen oxides and particulate matter (PM) but also greenhouse gas, which is typically carbon dioxide (CO_2) directly related to fuel consumption and vehicle efficiency. In respect of exhaust gas emissions, the upcoming emission regulation, EURO-6 restricts the level of NO_x and PM emissions for light-duty diesel vehicles [1].

In comparison of spark-ignition (SI) engine, diesel engine has proven to be superior to that of SI engine in terms of fuel consumption and torque for the last developing years. However, it has several drawbacks due to its combustion characteristic with high compression ratio. NO_x and PM is one of the problems [2]. Above all things, noise and vibration is widely known as a major representative issue of diesel engine in an aspect to passenger's drivability. Despite continued effort and the noise from diesel engine has been gradually decreasing, it is still an important problem [3]. Therefore, noise reduction has to be accomplished without loss of performance and any increase in exhaust emissions.

Conventional methodology to attain noise reduction depends on the rapid pressure rise in consequence of ignition delay and mixing condition of fuel and air [4]. Recent diesel engine normally operates under a number of parameters which affect to each other making various shape of heat release rate (HRR). Consequently, more discrete method to fulfil the noise reduction and other characteristics, such as exhaust gas emission, performance and fuel consumption.

1.1.2 Relationship between Combustion and Noise Emission

Primary cause of combustion noise in an internal combustion engine is known to be a rapid pressure rise in a chamber. Specifically, there are several categorized forms of combustion noise excitation, such as piston slap noise, crankshaft-induced noise which are generally classified indirect combustion noise [4]. Among them, only the noise caused by pressure excitation is defined as direct combustion noise.

In-cylinder pressure is directly affected by the combustion phenomena. There are mainly four phases of combustion in a conventional diesel engine. Figure 1-1 shows the ignition delay period, premixed, mixing-controlled, late combustion phase [5].

Ignition delay is defined as the period between the start of injection and combustion, which are expressed SOI and SOC respectively. Fuel begins to be injected into the combustion chamber after SOI. It is also mixed with air simultaneously for the chemical reaction which releases heat for work. The amount of premixed combustion is determined by the ignition delay because it is almost proportional to the mixing quantity. There are various factors influencing on the delay time, such as initial ambient temperature and pressure in chamber, mixing rate of fuel-air and fuel property, and cetane number [6].

Ignition delay can be divided into two parts, one is physical ignition delay and the other is chemical ignition delay [7]. Physical ignition delay is the time during atomization, evaporation and mixing with air entrained into the spray [8]. Chemical ignition delay is affected by the temperature, pressure, and the concentration of oxygen [9]. In an aspect of the heat release rate shape, peak of heat release rate and ignition delay have a strong relationship consequently.

The injection strategy of recent diesel engine introduces main fuel at near TDC. The first heat release phase, premixed combustion dominantly affects to the pressure rise. To be specific, in-cylinder pressure rise in a diesel engine can be divided into two parts, one is bulk rise, and the other is minor fall and rise near TDC. Bulk rise appears on the lower frequency range and attenuated by the engine block. Maximum pressure shows up also on these range. In respect of the excitation behavior within the middle range between 1 kHz to 3 kHz, it is important that the abrupt pressure increase which occurs when the premixed mixture burns as shown in figure 1-2 rather than the maximum pressure. It causes the second peak after TDC which is affecting to the combustion noise.

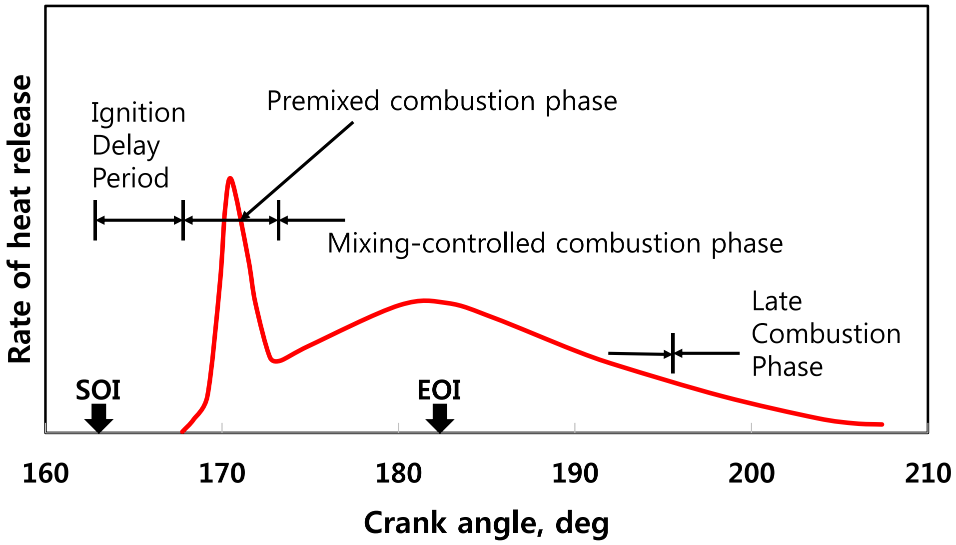

Figure 1-1. Heat release rate of conventional diesel combustion

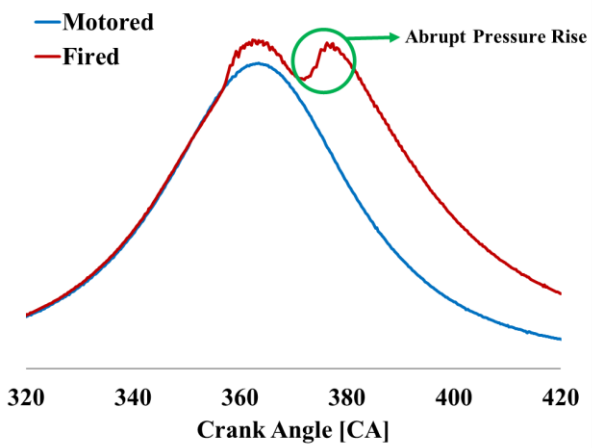

Figure 1-2. Abrupt pressure rise in a diesel engine combustion. Comparing to the motoring pressure curve, pressure rise occurs once more at near TDC due to the combustion.

1.2 Literature Review

1.2.1 Combustion Noise Reduction

Several papers have presented the relationship between combustion phenomena and noise emission.

Murayama et al. reversely calculated heat release rate from burning rate curve derived from Wiebe's function to estimate engine-out noise distribution of frequency range. Author found that peak pressure and MPRR are accompanied by a rapid increase in combustion noise. Maximum pressure was shown in low frequency range and the engine block commonly attenuates its level and less affect to combustion noise [10]. Recently, there are several studies for the engine development by using the simulated heat release rate [11, 12].

Badami et al. studied the effect of multiple injection strategies to various characteristics on a diesel engine. Two pilot and post injection were used. Noise reduction was achieved with the improvement of fuel consumption [13]. Hotta et al. revealed the pilot injection to decrease noise by empirical research regarding pilot injection timing and quantity. The increase in pilot injection ratio to main reduces noise level efficiently [14].

Mendez et al. studied also the multiple injection strategies effecting split heat release rate for decrease in peak of heat release rate (pHRR). This study effectively verified noise reduction by split injection lowering pHHR and widened HRR in advanced injection timing with lower compression ratio and high EGR corresponding to Premixed Charge Compression Ignition (PCCI) combustion mode. The location of pHRR in PCCI engine lies on near TDC, which is different conventional diesel engine having pHRR at after TDC causing increase in maximum pressure. Maximum pressure mainly affects to lower frequency in that the excitation source of noise emission and these frequency range commonly attenuated by engine block. In case of conventional diesel engine, pressure curvature near peak location is strongly related to the noise level more than that of maximum pressure [15]. Fuyuto et al. revealed the second injection effect of noise reduction in a PCCI diesel engine [16].

Shibata et al. found out the optimal point for noise reduction considering thermal efficiency in PCCI diesel engine. They also confirmed that noise reduction could be achieved with lower pHRR, in addition, combustion period and phase are closely related to noise level [17, 18]. However, only qualitative assessment was achieved in terms of related factors simultaneously. It is better to describe the effect and its quantitative approach of pHRR, combustion period and phase, respectively

There are many researches to reduce noise in respect of not only diesel combustion but also other noise sources, such as injector, flow noise and sound quality improvement.

Injector becomes one of the major cause of noise emission. Although gasoline engine has not a severe problem of noise comparing to that of diesel, it needs to improve the noise from the fuel injection system with the advance of Gasoline Direct Injection (GDI) engine. Many studies suggested the improvement of injector noise with high pressure pump [20-23]. Additionally, noise reduction methods from cam operation by analyzing cam seating velocity profile and flow of intake and exhaust manifold were studied also [19, 24]. In a diesel engine, the advancement in an aspect of sound quality has been studied. Several engines were evaluated by passenger and categorized [25]. Indices for indicating the emotion of drivers were developed [26, 27].

1.2.2 Indirect Noise Assessment Method

There are several methods to indicate combustion noise level without direct measurement. FEV suggested the index, Combustion Sound Level (CSL) for noise level caused by combustion process including piston slap, crank-shaft rotation and air mass effects [28]. Shahlari et al. introduced Combustion Noise Level (CNL) taking into account the structure attenuation and A-weighting, which represents human ear [29]. Commercialized indices are Lucas combustion noise meter and the AVL Noisemeter applying structural attenuation curve and cylinder pressure. Jung et al. proposed simplified index, Combustion Noise Index (CNI) that is only based on cylinder pressure by using one-third octave band. This is well-matched to the measured in the operation range from 1250 to 2000 rpm under various injection circumstances, such as main injection timing, injection pressure, pilot separation and its injection quantity [30].

Several researchers tried to estimate noise level without measuring noise directly by using noise index.

Torregrosa et al. studied the noise source diagnostic by in-cylinder pressure. Prediction of noise level from the pressure information has been more accurate than that of the block attenuation method which is conventional approach to identify the noise level [31].

Wang et al. had a use of AVL Noisemeter to optimize the combustion noise level in a diesel engine. There is a new structural attenuation curve for the improvement of reliability to measured noise level [32].

1.3 Objectives

Conventional approach to reduce combustion noise is focused on operating parameters and analyzing its measured data to find out the effect of each parameters. This study tried to figure out the methodology for noise reduction by simulating heat release rate. Due to the limitation of direct noise measurement, Combustion Noise Index (CNI) was used in this research as a direct combustion noise indicator. Pressure curve which is derived from the manipulated heat release rate was decomposed by frequency range to calculate CNI.

1. Derive design factors of heat release rate shaping by using simulated heat release rate. Based on the measured data, combustion phase, peak of heat release rate and combustion duration was changed to analyze CNI response.

2. Figure out experimentally the effect of combustion parameters to the shape of heat release rate. Exhaust gas emissions and bmep were also considered. Selected parameters would be used for the noise reduction process.

3. Verify the noise reduction by the experiment on the production engine with maintaining exhaust gas emissions and bmep. The effects of several combustion parameters were inspected in an aspect to the design factors.

Chapter 2. Effect of Heat Release Rate Shape to Combustion Noise

This chapter investigates the relationship between the shape of heat release rate and combustion noise by using Combustion Noise Index (CNI) as an indicator of noise level.

2.1 Combustion Noise Index

2.1.1 Difficulty of Measuring Direct Combustion Noise

Noise measurement of internal combustion engine is difficult to accomplish properly because of mainly two reasons. One is that it requires anechoic chamber which is high-priced and substantial spaced facility for the reliable measurement. The other results from the complexity of noise emission which is affected by lots of excitation sources through various transmitting paths. Engine noise can be divided into airborne and structure-borne noise which consists of three parts, one is mechanical, another is auxiliary and the other is combustion noise. Combustion noise is classified to direct and indirect combustion noise again as shown in figure 2-1 [3, 33].

Despite having relatively distinctive along the time and frequency range from some of sources, almost all of them is still difficult to be decomposed properly by measuring noise level outside of the engine [34]. Additionally, combustion-related noise comprises huge proportion of total emission [35, 36]. Therefore, in-cylinder pressure as the main excitation source is necessarily focused on in an aspect to noise reduction. CNI is proper index to represent direct combustion noise considering only in-cylinder pressure. It is well-matched to the measured noise level and easy to calculate [30].

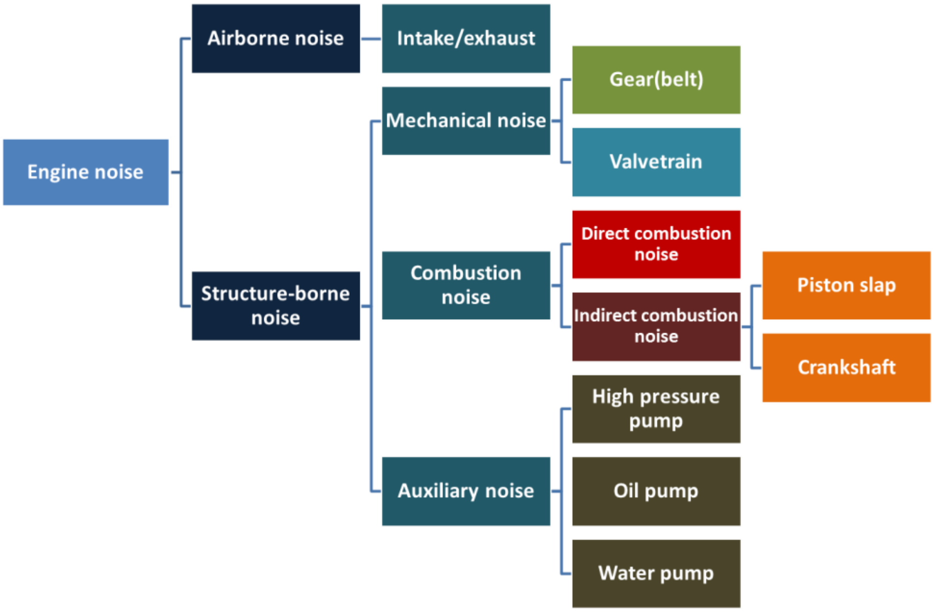

Figure 2-1. Engine noise classification. Engine-out noise is hard to be decomposed by each component in that it is the output of a number of sources.

2.1.2 Calculation of Combustion Noise Index

Direct combustion noise is generated by only in-cylinder pressure excitation. Conventional light duty diesel engine shows significant frequency distribution in range of below 5 kHz. These excitation force is transmitted through the engine block and emitted in a form of noise. Block has attenuation characteristics, relatively strong on the high and low frequency range [37]. Middle range from about 1 kHz to 3 kHz becomes major source of direct combustion noise in that the excitation force in these range is less attenuated by the engine block.

Jung et al. introduced CNI which is the index to represent direct combustion noise level by using only cylinder pressure level [30]. One-third octave band approach is one kind of classical approach to calculate the level of combustion noise [38].

it is widely used for analyzing noise level by frequency ranges. It is an appropriate approach of noise assessment in a view of energy. The equations defining a one-third octave system are listed below [39].

1. The ratio of center frequency(C.F) of the $(i)^{th}$ to the $(i{+}N)^{th}$ one-third octave:

$$\frac{(C.F.)_{i+N}}{(C.F.)_i} = 2^{N/3}$$

2. The ratio of the bandwidth (B.W.) of the $(i)^{th}$ octave to the $(i{+}N)^{th}$ one-third octave:

$$\frac{(B.W.)_{i+N}}{(B.W.)_i} = 2^{N/3}$$

3. The lower limit frequency (f_L) of any given one-third octave:

$$f_L = \frac{(C.F.)}{2^{1/6}}$$

4. The upper limit frequency (F_u) of any given one-third octave:

$$f_u = 2^{1/6}(C.F.)$$

According to the below equation, CNI can be computed by the summation of center frequency levels between 1 kHz and 3.15 kHz of one-third octave band. The procedure is depicted in figure 2-2.

$$\text{CNI [dB]} = 10 * \log(\sum_{1kHz}^{3.15kHz} 10^{(Center\ freq.\ level)/10})$$

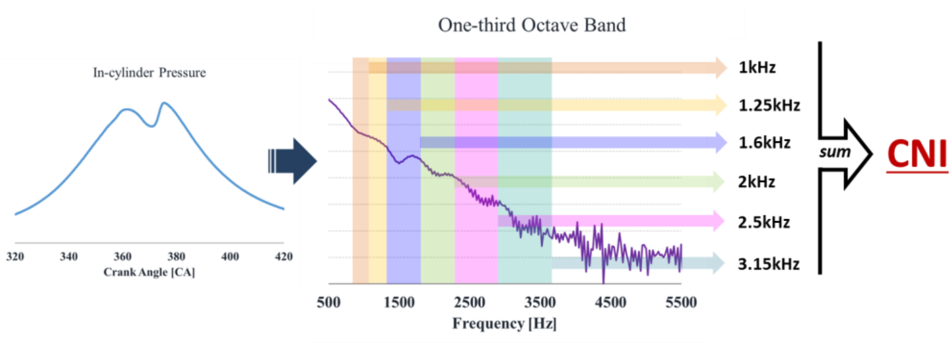

Figure 2-2. CNI calculation procedure. In-cylinder pressure data with an accurate time interval is decomposed by frequency-magnitude by fast fourier transform. Continuous frequency-magnitude data transforms to the discrete form by 1/3 octave processing method. Finally, CNI is computed in result of summation.

2.2 Experimental Setup

Simulated heat release rate is based on the measured data by experiment. This chapter describes specific test and measurement instrument for the subject engine operation. Schematic diagram of overall experimental setup is shown in figure 2-3.

A production engine which has an in-line 4 cylinder 1.6L diesel engine with common rail system for Euro5 regulation was used for the experiment. Fuel is injected by piezoelectric type injector with high pressure as shown in table 2-1. The engine was coupled with AC dynamometer for the control and measurement of speed and torque. The dynamometer specifications are listed in table 2-2. Coolant temperature was controlled while the engine is on operation by electric controller. Fuel was supplied by fuel pump with temperature controller maintaining 40℃. Ambient temperature was controlled to 25℃ by air-conditioning system in the test cell by supplying air to the engine inlet.

Smoke meter measures PM in FSN (Filtered Smoke Number) during steady operation. The specifications of smoke meter are on table 2-3. Exhaust gases were analyzed by HORIBA MEXA-7100DEGR for NO and EGR ratio. EGR ratio was calculated by measuring CO_2 fraction of intake and exhaust manifolds. The measurement principles of exhaust gas analyzer are listed in table 2-4.

For the data acquisition and combustion analysis, KiBox 2893A was used. As mentioned above, piezoelectric pressure sensor emits charges and transmits into charge amplifier in KiBox. The measured data is arranged along the crank angle domain which is calculated from crank position sensor on the engine by combustion analyzer. The specifications of combustion analyzer are listed on table 2-5.

The measurement of in-cylinder pressure is important because CNI calculation is based on the measured pressure data. Glow-plug type piezoelectric pressure sensor (Kistler 6056A) was installed in the first cylinder. Its signal is transmitted to the charge amplifier in KiBox and measured. Measuring frequency is 312.5 kHz with the accurate time interval. With the crank angle domain, cyclic in-cylinder pressure data was gathered. CNI was computed by using the data in a range of -180 ^{o} to 180 ^{o} aTDC. In addition, the number of sample affects to the level of CNI. It is down-sampled to 52.1 kHz and controlled by 2048. The specifications of pressure sensor are shown in table 2-6.

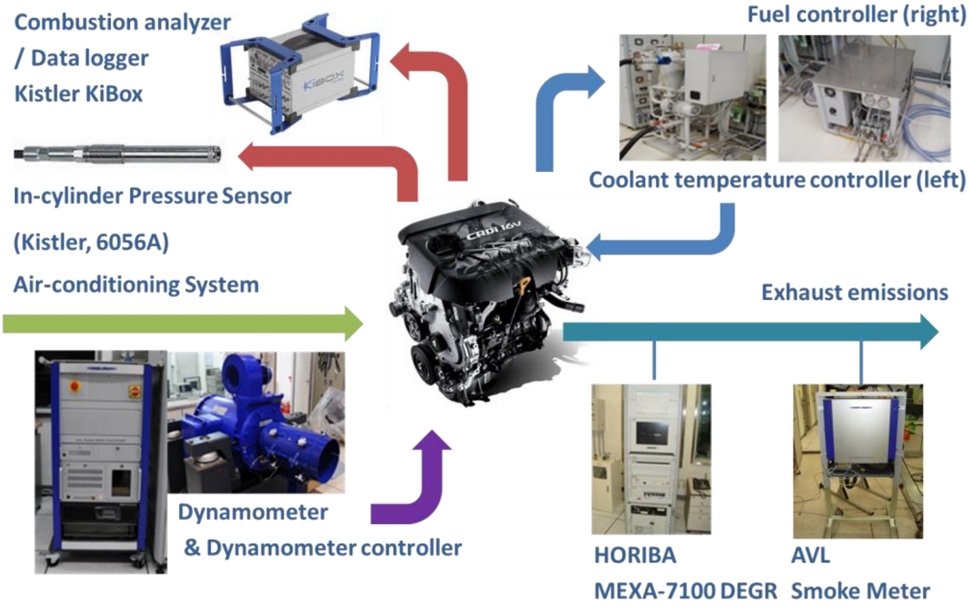

Figure 2-3. Schematic diagram of engine experiment and measurement instrument. In-cylinder pressure sensor is installed on the glow-plug site by using specially designed adaptor.

Table 2-1. Engine specifications

Engine Type	Inline 4 cylinders, DOHC
Displaced volume	1582 cc
Bore X Stroke	77.2 mm X 84.5 mm
Compression ratio	17.3:1
Injector type	Bosch Solenoid Injector
Maximum power	94 kW @ 4000 rpm
Maximum torque	26.5 kg.m @ 1900~2750 rpm
Emission regulation	Euro5

Table 2-2. Specifications of dynamometer

Item	Specification
Manufacturer	AVL
Model	Alpha 240
Capacity	240 kW
Type	Eddy Current
Maximum speed	10,000 rpm
Maximum torque	600 N·m
Measurement accuracy	Torque: ±0.2% Speed: ±1 rpm
Cooling type	Air Cooling

Table 2-3. Specifications of smoke meter

Item	Specification
Manufacturer	AVL
Model	AVL 415S
Measurement range	0 to 10 FSN 0 to 32,000 mg/m^3
Resolution	0.001FSN 0.01 mg/m^3
Repeatability (at standard deviation)	$\sigma \leq \pm$ (0.005 FSN + 3% of measured value)
Reproducibility (as standard deviation)	$\sigma \leq \pm$ (0.005 FSN + 6% of measured value)

Table 2-4. Measurement principle of emission analyzer (MEXA-7100DEGR)

Emission Gas	Measurement Principle
NO_x	Chemiluminecent Detector
THC	Flame Ionization Detector
O_2,CO_2,CO	Non Dispersive Infrared Rays

Table 2-5. Specifications of combustion analyzer with data logger

Basic Description	
Manufacturer	Kistler
Model	KiBox® To Go 2893A
Amplifiers type	5064C12
Ambient Conditions	
Temperature range	- 30 – 50℃
Relative humidity	0 – 95% non-condensing
Power supply	10 – 36 VDC, 100 – 250 VAC
Power consumption	approx. 60W
Charge Amplifier	
Number of channels	4 (2-channels each, 2 amplifiers)
Measuring range	±100 – 100,000 pC
Output voltage	0 – ±10 V
Output current	0 – ±2 mA
Analog Input Channels	
Number	8 channels
Input voltage range	-10 – 10 V
ADC resolution	16-bit
ADC sample rate	1.25MHz (MS/s) per channel 312.5 kS/s for the use of data logger
Low-pass filter	Off/5/10/20/25/30/35/40 kHz

Table 2-6. Specifications of piezoelectric pressure sensor

Technical Data	
Operating temperature	- 40 – 140℃ (max. 150℃)
Pressure range	0 – 200 bar (max. 210 bar)
Sensor	
Power supply (V_{dd})	5,0V or 3,3V
Output signal	Ratio metric
Bandwidth	0 to 5 kHz
Accuracy	±2%
Glow Function	
Current 60sec	< 10A
Temperature after 60sec	> 980℃
Max. temperature	1100℃

2.3 Experimental Conditions

Simulated heat release rate in this study is based on the measured data which is acquired at the engine speed of 1500 rpm and the fuel amount of 15 mg/hub as shown in table 2-7.

Four combustion parameters were selected so as to design heat release rate. These are main injection timing, injection pressure, swirl ratio, and EGR ratio.

Main injection timing directly influences on not only the combustion phase but also the ignition delay due to the change of in-cylinder temperature and pressure. Conventional injection strategy occurs at near TDC. Advancing injection timing near TDC shortened ignition delay by locating initial fuel to highly compressed air. pHRR decreases with low premixed mixture.

Fuel injection pressure affects to the physical ignition delay. Higher injection pressure makes initial fuel particles better to evaporate reducing ignition delay and PM emission. Additionally, it reduces injection. Consequently, pHRR increases and phase is advanced.

Swirl motion in chamber strongly affects the physical ignition delay also, especially mixing condition. pHRR increases with the same combustion phase as strengthened air flow gives better evaporation and mixing with air.

Lastly, EGR ratio has influence on burning rate and ignition delay. Lowering oxygen concentration in the mixture retards chemical ignition process by increasing pHRR with further combustion phase.

Table 2-7. Base operating condition

Variables	Unit	Value
Engine speed	[rpm]	1500
Torque	[N·m]	68.6
bmep	[bar]	5.45
Ambient temperature	[deg]	21.43
Temperature after IC	[deg]	37
Coolant temperature	[deg]	90
Total fuel quantity	[mg/hub]	15
Pilot1 quantity (second)	[mg/hub]	1.3
Pilot2 quantity (first)	[mg/hub]	1
Main injection quantity	[mg/hub]	12.7
Main injection timing	[bTDC CAD]	3
Pilot1 timing	[bTDC CAD]	13
Pilot2 timing	[bTDC CAD]	23
Rail pressure	[bar]	500
Swirl	[%]	95
EGR ratio	[%]	24.49
Boost pressure	[hPa]	1098
Equivalent ratio	[-]	0.75
Mass flow rate of air	[mg/hub]	285
Humidity	[%]	30.9
NO	[ppm]	146.09
PM	[FSN]	3.702
THC	[ppm]	154.85
CNI	[dB]	171.76

2.4 Process of Heat Release Rate Simulation

Based on the measured pressure data under 1500 rpm and 15 mg/hub, inverse operation from burning rate or heat release rate is achieved to derive in-cylinder pressure. In figure 2-4 (a), blue line which represents the base condition was extended with the same time domain. Heat release rate is the first derivation of burning rate. Finally, in-cylinder pressure curve can be obtained from heat release rate. For example, figure 2-4 (b) represents slower combustion phenomenon.

Traditional single-zone First Law equation was used in this paper neglecting heat loss with several proper assumptions [40-45].

$$\mathrm{dQ} = \frac{\gamma}{\gamma - 1} p dV + \frac{1}{\gamma - 1} V dp$$

where Q is the gross released heat, γ is the specific heat ratio. p is the in-cylinder pressure, V is the cylinder volume. The above equation for the calculation of heat release rate is an approximation because uniform temperature, pressure and ideal gas in cylinder were assumed. Subsequent to this, mean specific heat is taken with the assumption of narrow temperature variation. In result, γ is assumed to be constant. After manipulating heat release rate, p is calculated inversely.

There are mainly three parts followed. First, combustion phase was varied with the same shape of HRR. Second, pHRR variation. Lastly, width of HRR which is related to combustion duration was examined.

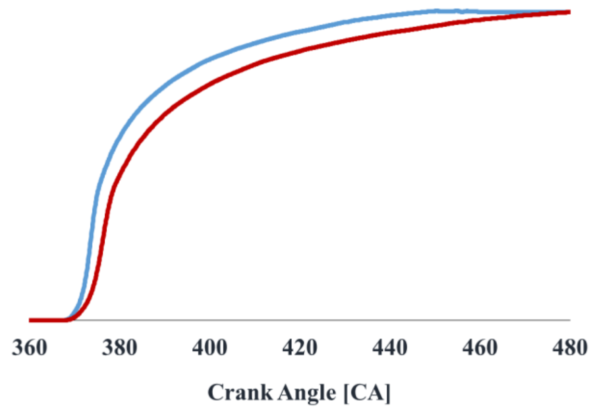

(a)

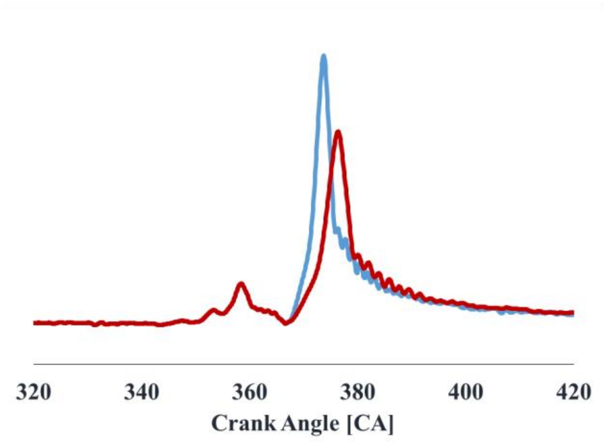

(b)

Figure 2-4. Process of heat release rate simulation of (a) burning rate and (b) manipulated heat release rate. Simulated heat release rate is derived from the extended burning rate from the base curve. It represents the slow combustion under the same fuel quantity.

2.5 Design Factors for Noise Reduction

This chapter suggests three design factor which affect to CNI: Combustion phase, pHRR and width of heat release rate. In contrast with the real combustion, identical HRR shape was used for the combustion phase effect. In case of peak and width of HRR, the shape is linearly scaled with different area which represents the quantity of introduced fuel amount. Entire process is based on the measured data of 1500 rpm and 12.94 mg/hub of main fuel injection quantity. The width of heat release rate is defined as a duration between SOC and the location of pHRR to focus on the premixed combustion.

CNI increases with the advanced combustion phase in the figure 2-5. With the advance of combustion phase, cylinder volume at the combustion decreases affecting to the pressure rise rate. The location of pHRR was advanced by 5 CAD with the same pHRR and premixed duration as shown in table 2-8.

When combustion phase is advanced before TDC, curvature between two peaks of pressure curve becomes smoothed for frequency range moving towards that of low frequency. Generally, engine block attenuates except between 1 kHz and 3 kHz. Therefore, maximum pressure is less effective to noise level because of attenuation by block and peak-to-peak curvature shape is more important than maximum pressure shown in figure 2-6. CNI decreases with the advanced combustion phase as shown in table 2-9.

Under the same combustion phase, pHRR decreases with lower CNI. Lower pHRR affects to the second peak pressure curve lying down referred to figure 2-7. The location of pHRR is closely related to the maximum pressure rise rate. Higher pHRR indicates the slope of pressure on the second peak becomes stiff. Main fuel quantity increases from 10.73 to 15.14 mg/hub as shown in table 2-10.

Lastly, wider heat release rate reduces CNI even with the higher accumulated heat. Wide heat release rate represents the slow combustion affecting to the smoother pressure rise in chamber as shown in figure 2-8. The width of heat release rate, especially premixed period, could be expressed by using the duration of the first slope because rear part of heat release rate contains diffusive combustion. Main fuel quantity increases from 12.06 to 15.27 mg/hub as shown in table 2-11. CNI decreases even with the increased fuel injection quantity.

Consequently, there are three design factors of heat release rate shape; which affect to the pressure curve and combustion noise in order. Advance of combustion phase, higher pHRR and reduced combustion duration function as the increase factors to CNI.

Practical heat releasing phenomena shows the close correlation between peak of heat release rate and that of the width. As mentioned in the previous chapter, major source of direct combustion noise is rapid pressure rise during the premixed combustion. The quantity of premixed burned fuel is directly affected to the mixing condition. After fuel is introduced, the required time until the ignition dominantly determines the fuel-air mixing. Mixing fuel with sufficient air increases pHRR under the same combustion duration.

Table 2-8. Results of phase shifting

Speed	Fuel(main)	Max.dQ CA	imep	Max. dQ	SOC	Duration	CNI
[rpm]	[mg/hub]	[aTDC CAD]	[bar]	[J/deg]	[aTDC CAD]	[CAD]	[dB]
1500	12.94	3.95	7.12	68.50	-2.80	6.74	180.13
	12.94	8.97	6.85	68.50	2.21	6.76	179.36
	12.94	13.97	6.51	68.50	7.24	6.73	178.14
	12.91	18.91	6.14	68.50	12.16	6.76	176.60
	12.83	23.96	5.71	68.50	17.17	6.79	174.84

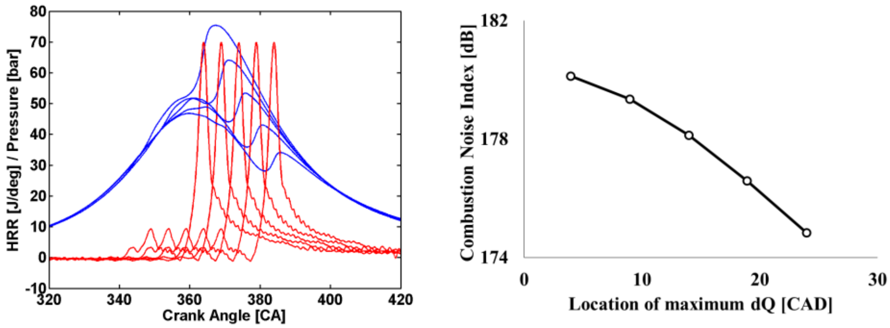

Figure 2-5. Advance of combustion phase. Conversely, HRR is retarded by 5 CAD under the same pHRR and premixed duration (left). CNI decreases with the retarded phase (right).

Table 2-9. Results of further phase shifting before TDC

Speed [rpm]	Fuel(main) [mg/hub]	Max.dQ CA [aTDC CAD]	imep [bar]	Max. dQ [J/deg]	SOC [aTDC CAD]	Duration [CAD]	CNI [dB]
1500	12.91	-16.03	7.18	68.50	-22.80	6.76	174.63
	12.92	-11.02	7.31	68.50	-17.77	6.75	177.20
	12.92	-6.09	7.34	68.50	-12.83	6.75	178.97
	12.92	-1.07	7.28	68.50	-7.81	6.74	179.94
	12.94	3.95	7.12	68.50	-2.80	6.74	180.13

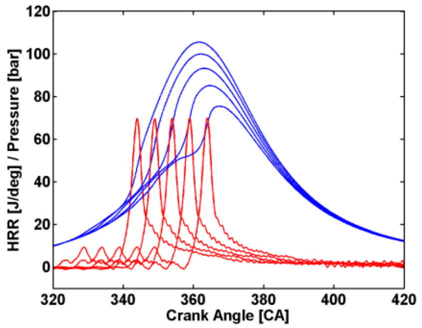

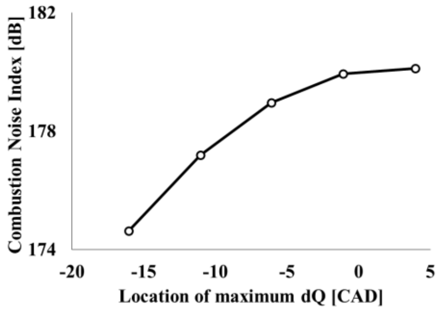

Figure 2-6. Further phase advance to bTDC. CNI decreases although maximum pressure goes higher in result of phase advance. Maximum pressure affects to the low range under 800 kHz which is out of summation range for computing CNI. Low frequency sources are normally attenuated by the engine block.

Table 2-10. Results of pHRR change

Speed [rpm]	Fuel(main) [mg/hub]	Max.dQ CA [aTDC CAD]	imep [bar]	Max. dQ [J/deg]	SOC [aTDC CAD]	Duration [CAD]	CNI [dB]
1500	10.73	13.62	5.37	54.85	6.89	6.73	176.16
	11.83	13.62	5.94	61.70	6.89	6.73	177.27
	12.93	13.62	6.52	68.56	6.98	6.65	178.20
	14.04	13.62	7.09	75.42	6.98	6.65	179.04
	15.14	13.62	7.66	82.27	6.98	6.65	179.80

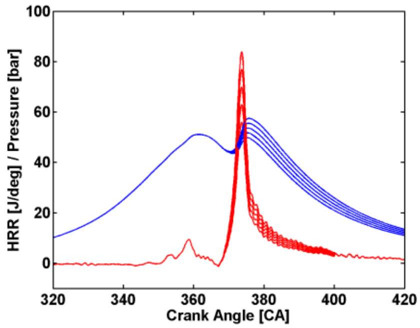

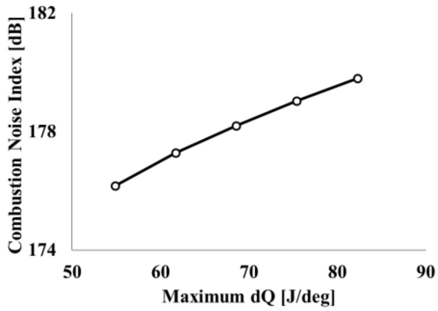

Figure 2-7. Decrease in peak of heat release rate. pHRR decreases with the change of fuel quantity. CNI decreases with lower pHRR.

Table 2-11. Results of widened heat release rate

Speed [rpm]	Fuel(main) [mg/hub]	Max.dQ CA [aTDC CAD]	imep [bar]	Max. dQ [J/deg]	SOC [aTDC CAD]	Duration [CAD]	CNI [dB]
1500	12.06	13.71	6.06	68.51	7.76	5.95	178.41
	12.93	13.62	6.52	68.56	6.98	6.65	178.20
	13.72	13.62	6.92	68.54	6.28	7.34	177.98
	14.49	13.54	7.33	68.55	5.59	7.94	177.74
	15.27	13.54	7.74	68.56	4.90	8.64	177.49

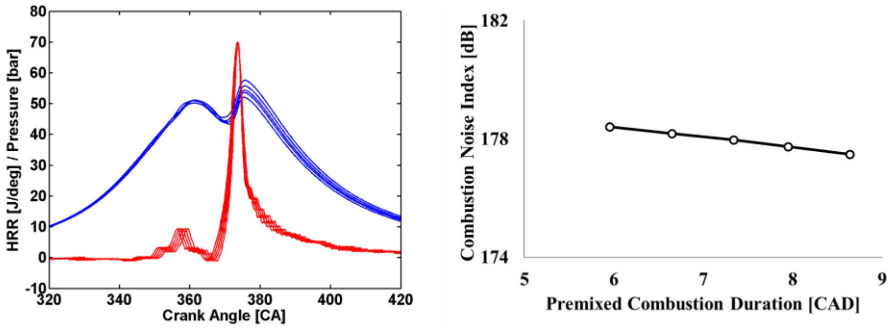

Figure 2-8. Widened heat release rate. It represents the slowly-burned combustion. CNI decreases with wider heat release rate even though the total amount of fuel increases.

Chapter 3. Noise Reduction by Heat Release Rate Shaping

This chapter shows firstly the effect of combustion parameters on CNI and the shape of heat release rate. Additionally, exhaust gas emissions and bmep were also considered to confirm the effect of various combustion parameters. Combustion phase is generally expressed the location when the total injected fuel burns 50% mass. In this study, the location of pHRR was used instead of CA50 to focus on the premixed combustion.

Second, noise reduction in respect of heat release rate shape by applying suggested three design factors, combustion phase, pHRR and width of heat release rate were introduced. From the base condition, combustion parameters were varied. The level of design factors were inspected simultaneously whether these factors change towards the decrease in CNI under the maintained exhaust gas emissions and bmep.

3.1 Effect of Combustion Parameters on Combustion Noise Index

First of all, several combustion parameters were varied to confirm the response to heat release rate and CNI. Four combustion parameters were manipulated in a view of aspect ratio and combustion phase in order that CNI decreases with maintaining exhaust gas emissions and bmep.

Injection timing from -3 to 3 bTDC CA shows significant reduction of CNI with widened HRR, lower pHRR shown in figure 3-1. When the phase advance until 3 bTDC CA, main fuel is injected at higher temperature and pressure condition causing worsening fuel and air mixing condition. Then, HRR becomes wider with lower pHRR. NO level is higher and PM decreases due to the increase in maximum temperature and pressure. bmep increases for the same reason.

Fuel injection pressure from 600 to 400 bar decreases CNI with widened HRR, retarded combustion phase and lower pHRR shown in figure 3-2. Reduced rail pressure have negative effect on fuel and air mixing condition. Burning rate of premixed fuel decreases. Decrease in injection pressure affects to the worse evaporation resulting the increase in PM emission and the decrease in NO. bmep increases slightly.

EGR ratio from 30 to 20% results the decrease in combustion noise with widened HRR, lower pHRR, advanced combustion phase. Ignition delay is reduced due to the increase in oxygen concentration with the decrease of EGR ratio. In contrast, less EGR increases temperature on the flame surface with higher NO. PM decreases simultaneously with lower equivalence ratio as shown in figure 3-3.

Swirl valve from 95 to 60% in chamber significantly decreases CNI with widened HRR and lower pHRR as shown in figure 3-4. Swirl motion in chamber affects to the mixing condition and premixed burned fuel quantity.

Pilot injection quantity 1 to 1.6 mg/hub results the decrease in CNI with widened HRR and lower pHRR as shown in figure 3-5. By increasing pilot quantity near main injection, temperature rises at the time when main fuel begins to be injected. It reduces the mixing ratio of fuel and air lowering pHRR.

Table 3-1. Experimental conditions

<table>
<tr><th>Engine Speed

[rpm]</th><th>Total Fuel

[mg/hub]</th><th>Main Injection Timing

[bTDC CA]</th><th>Rail Pressure

[bar]</th><th>Swirl

[%]</th><th>EGR

[%]</th><th>Pilot1 Quantity

[mg/hub]</th></tr>
<tr><td rowspan="11">1500</td><td rowspan="9">15</td><td>0</td><td rowspan="3">500</td><td rowspan="5">95</td><td rowspan="7">25</td><td>1.3</td></tr>
<tr><td>-3</td><td rowspan="8"></td></tr>
<tr><td>3</td></tr>
<tr><td rowspan="8">0</td><td>600</td></tr>
<tr><td>400</td></tr>
<tr><td rowspan="6">500</td><td>80</td></tr>
<tr><td>60</td></tr>
<tr><td rowspan="4">95</td><td>20</td></tr>
<tr><td>30</td></tr>
<tr><td>15.3</td><td rowspan="2">25</td><td>1.6</td></tr>
<tr><td>14.7</td><td>1</td></tr>
</table>

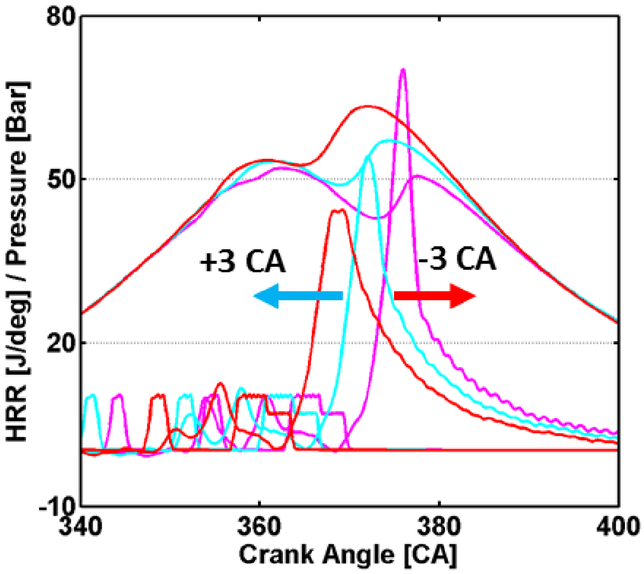

(a)

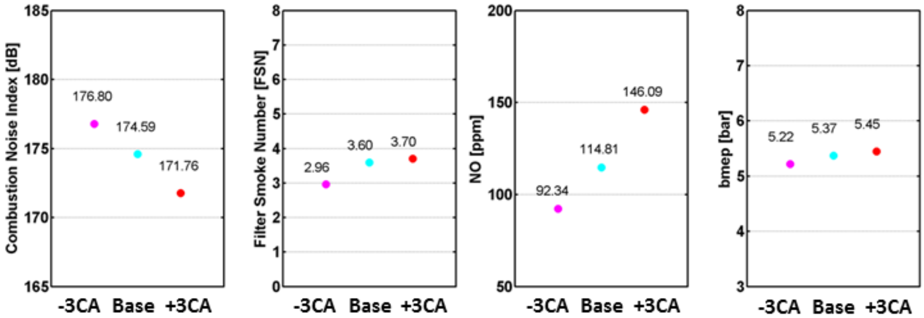

(b)

Figure 3-1.Effect of Injection timing described by (a) pressure and heat release rate, pressure rise rate (b) CNI, PM, NO and bmep respectively. Each case is depicted by the same color. Trapezoidal signal shows the injection signal shown in (a).

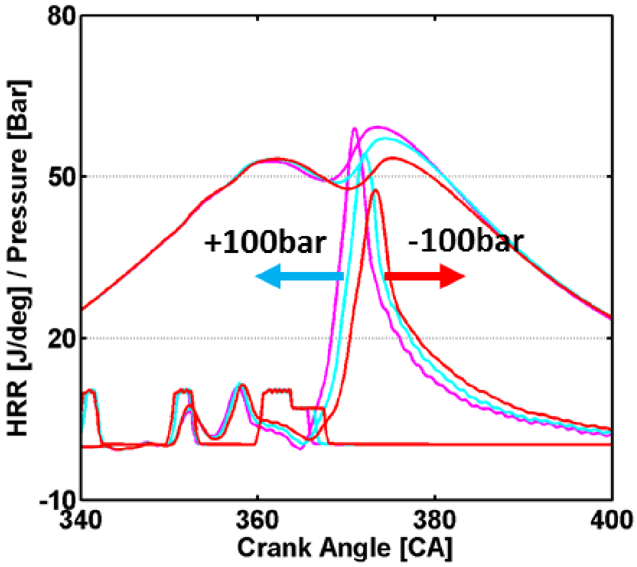

(a)

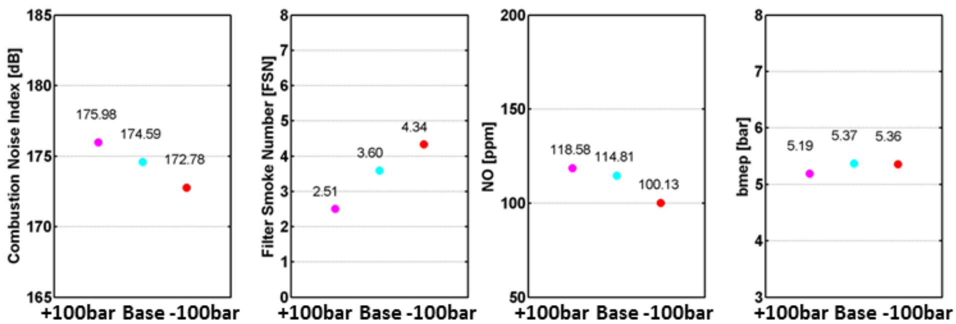

(b)

Figure 3-2. Effect of njection pressure described by (a) pressure and HRR (b) CNI, PM, NO and bmep. Each case is depicted by the same color. Trapezoidal signal shows the injection signal shown in (a).

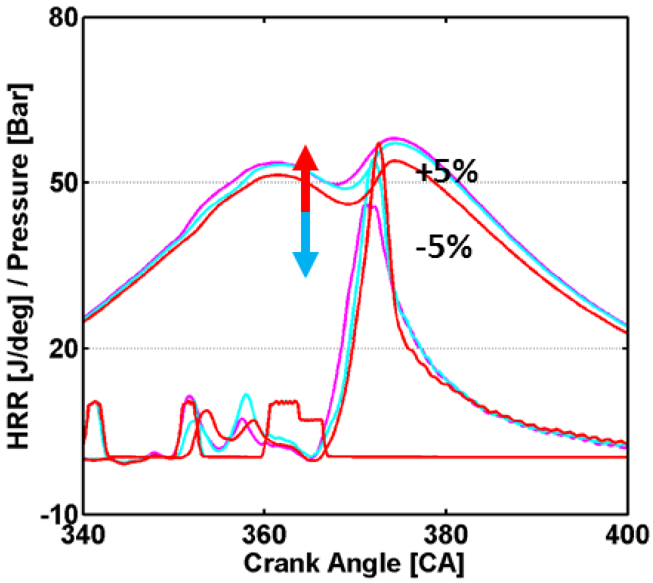

(a)

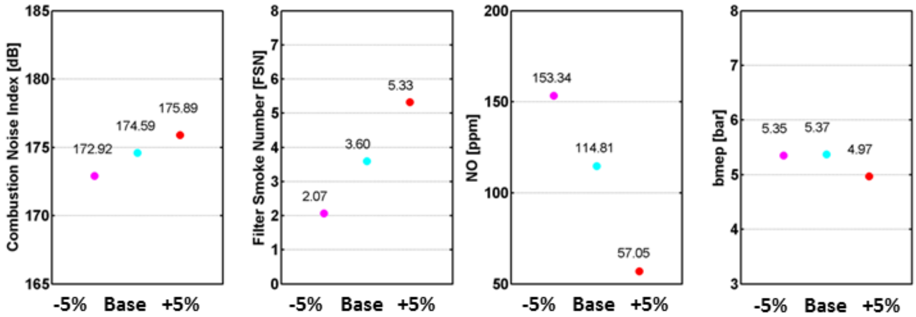

(b)

Figure 3-3. Effect of EGR ratio described by (a) pressure and HRR (b) CNI, PM, NO and bmep. Each case is depicted by the same color. Trapezoidal signal shows the injection signal shown in (a).

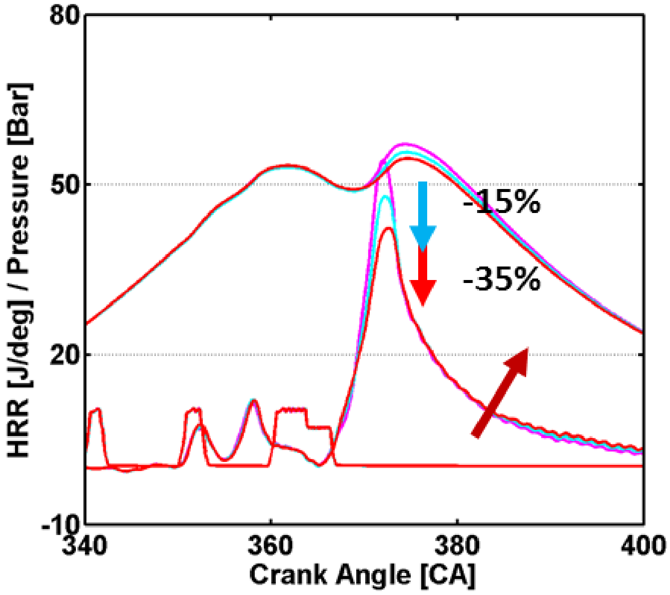

(a)

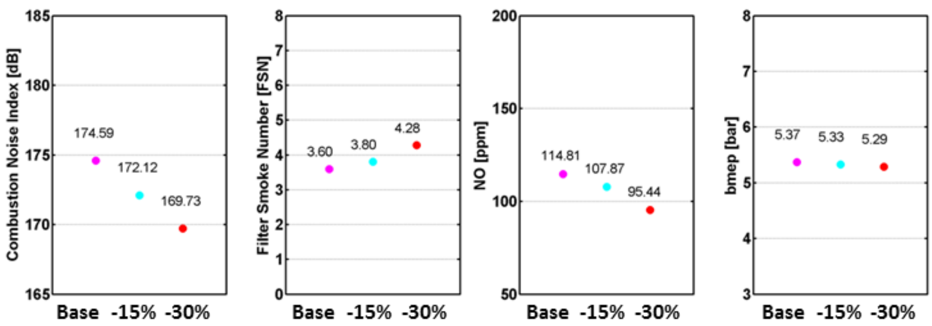

(b)

Figure 3-4. Effect of swirl motion described by (a) pressure and HRR (b) CNI, PM, NO and bmep. Each case is depicted by the same color. Trapezoidal signal shows the injection signal shown in (a).

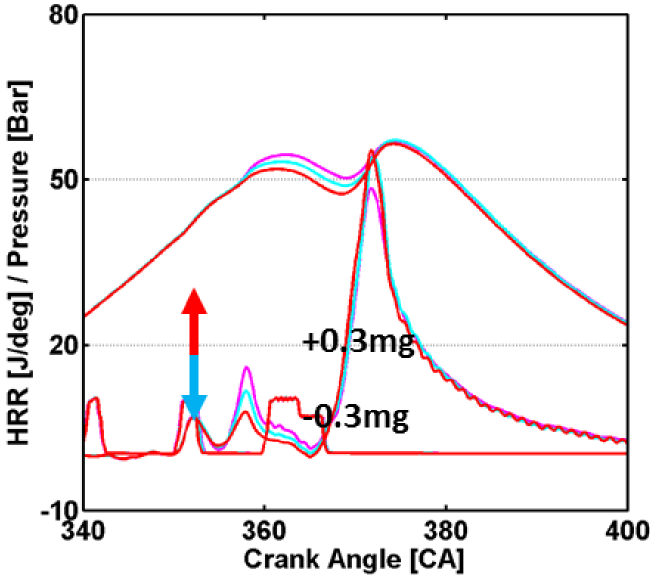

(a)

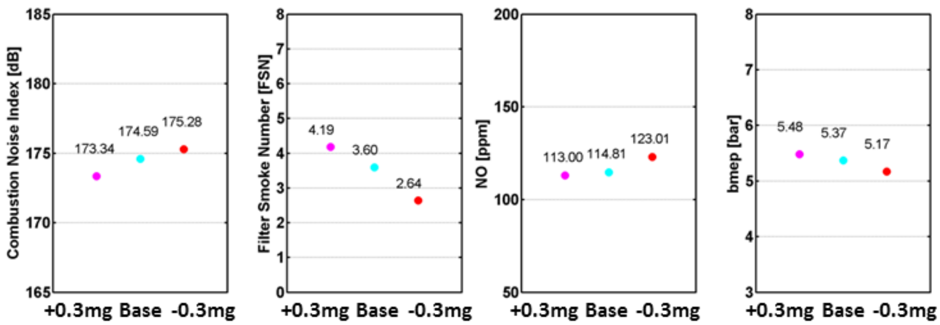

(b)

Figure 3-5. Effect of pilot quantity described by (a) pressure and HRR (b) CNI, PM, NO, bmep. Each case is depicted by the same color. Trapezoidal signal shows the injection signal shown in (a).

3.2 Noise Reduction Considering Exhaust Gas Emission and bmep

Noise reduction was achieved with decreased NOx and PM. The experiment was conducted from the base condition as changing four parameters and its responses to three design factors, which are the combustion phase, pHRR and width of heat release rate. While the CNI reaches to the lower level considering exhaust gas emissions and bmep, entire procedure is categorized into three steps. The first step is the retard of main injection timing and reduced swirl. Second, injection pressure was reduced. Lastly, EGR ratio decreased.

3.2.1 Retard of Main Injection Timing and Reduced Swirl

Starting from the base operation #1 in table 3-2, combustion phase moves backwards by retarding main injection timing until TDC. According to the result of chapter 3.1, retard of injection timing affects to the higher pHRR. Swirl motion was suppressed to cope with pHRR increase in consequence of retarded injection timing (#2). Swirl valve in front of two intake ports for one cylinder controls the swirl motion by blocking one port stream for stratified intake air flow. As a result of changing these parameters, pHRR CA varied from 9.2^{o} to 12.2^{o} aTDC. In contrast, pHRR increases from 44.4 to 47.9. Duration does from 7.5 to 7.1 CAD. Although combustion phase was retarded, pHRR becomes higher; and width becomes widened. Consequently, CNI increases. In respect of exhaust gas emission and bmep, NO decreases with lower maximum pressure; and bmep decreases as shown in figure 3-6, 7.

3.2.2 Decrease in Injection Pressure

Figure 3-7 shows that the retard of phase cannot successfully achieve noise reduction because of increase in pHRR with shortened duration. As from the operation

#2 to #3, injection pressure was reduced for 100 bar. pHRR decreases and combustion duration becomes longer shown in figure 3-8. Consequently, pHRR CA was retarded from 12.2 to 13.6; and pHRR was varied from 47.9 to 44.0. Duration increases from 7.1 to 7.7. CNI decreases from 172.1 to 170.9. NO was reduced drastically until 61.5% of base condition. In contrast, decrease in injection pressure has a negative influence on PM from 3.8 to 5.1 FSN shown in figure 3-6.

3.2.3 Reduced EGR Ratio

As a result of second approach by lowering injection pressure, tremendous particulate matters were measured. Instead of decreasing injection pressure which reduces pHRR, lower EGR ratio and weakening swirl motion were introduced in sequence. pHRR decreases as shown in figure 3-9. Lower EGR influences on the ignition delay by increasing oxygen concentration. Premixed combustion duration decreases from 7.7 to 7.5 which is the same level of the base condition (#1). Combustion phase is slightly advanced from 13.6 to 12.6 which is retarded by 3.4 CAD. pHRR decreases from 44.0 to 40.7 which is decreased by 3.7. Consequently, CNI decreases by 3.6 dB until 168.1 as shown in figure 3-6.

Table 3-2. Combustion parameters of the noise reduction process

Experiment	Main injection timing [bTDC CAD]	Rail Pressure [bar]	Swirl [%]	EGR [%]
#1	**3**	**500**	**95**	**24.49**
#2	**0**	**500**	**80**	**24.57**
#3	**0**	**400**	**80**	**24.28**
#4	**0**	**500**	**60**	**20**

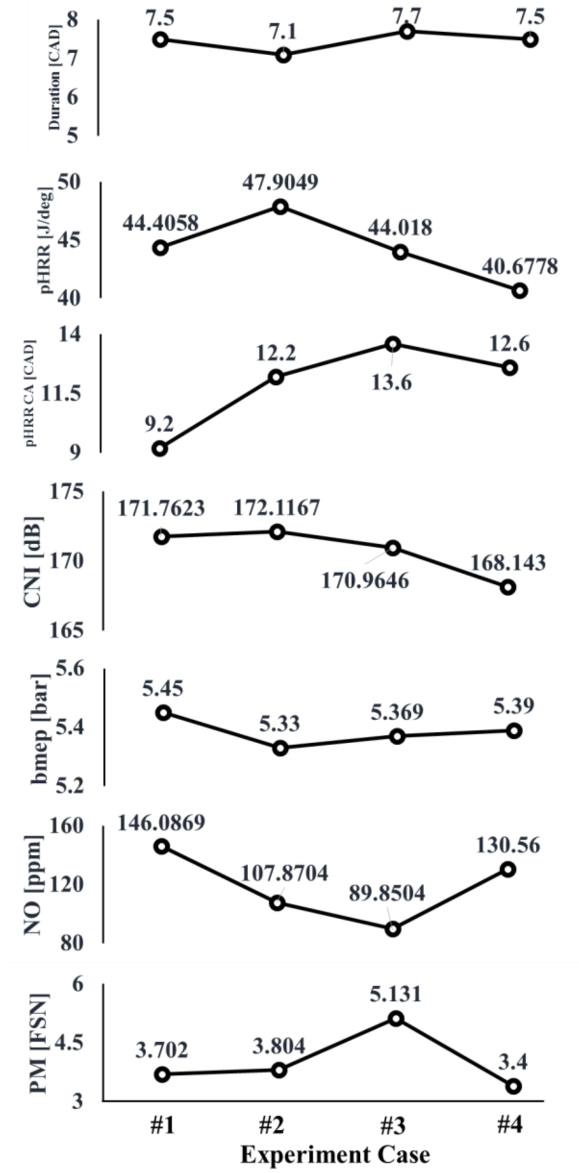

Figure 3-6. Design factors and characteristics of noise reduction process. Entire experiments is conducted from #1 to #4 for noise reduction. It is divided by 4 steps which are depicted on the figure. Engine speed: 1500 rpm; Fuel quantity: 15 mg/hub

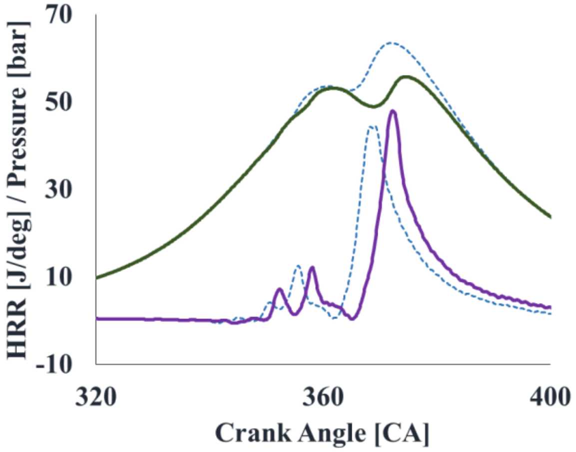

Figure 3-7. Retarded combustion phase and reduced swirl motion in chamber. Dotted plot indicates the previous case (#1) and solid line of the present case (#2).

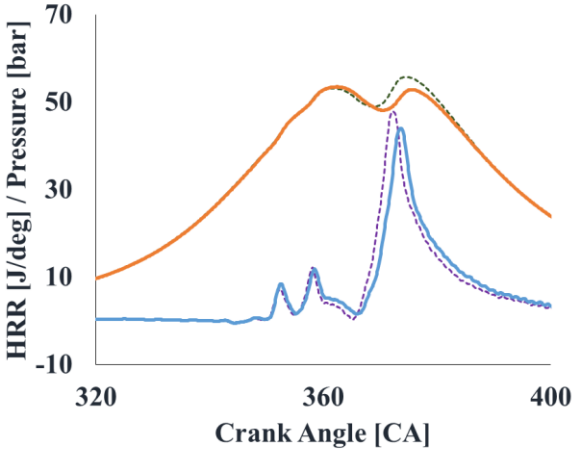

Figure 3-8. Reduced injection pressure. Dotted plot indicates the previous case (#1) and solid line of the present case (#2).

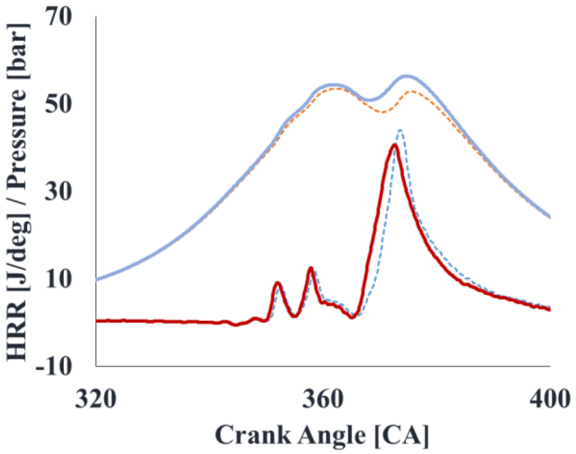

Figure 3-9. Reduced EGR ratio and swirl motion. Dotted plot indicates the previous case (#1) and solid line of the present case (#2).

Chapter 4. Conclusion

In this research, new approach to reduce combustion-induced noise was verified. Combustion Noise Index was used for the combustion noise indicator in this study instead of measuring combustion noise. The effect of heat release rate shape on CNI was investigated. The design factors were derived for heat release rate shaping. Experiments for noise reduction were conducted by using these design factors considering exhaust gas emissions and bmep.

The shape of heat release rate affects to CNI. There are three design factors which determine the shape of heat release rate: Combustion phase, pHRR, width of heat release rate. First, CNI decreases in case of retarded combustion phase. To be specific, CNI becomes lower when the combustion phase is shifted far from TDC, which maximizes compression ratio. Maximum pressure shows relatively less correlation with CNI. Second, CNI decreases with lower pHRR. Lower peak of heat release rate influences on the maximum pressure rise rate, which indicates the slope of abrupt pressure increase on the second pressure peak. Finally, wider heat release rate reduces CNI even with the higher fuel quantity. In case of the real operation, slow combustion under the same fuel amount shows not only the increase of width but also the decrease in pHRR.

There are five combustion parameters were verified in respect of the above three design factors with exhaust gas emission and bmep. Combustion parameters are injection timing, pressure, swirl ratio, EGR ratio and pilot quantity.

Retard of injection timing shows higher pHRR, narrowed HRR width and retarded combustion phase. CNI increases. Higher pHRR affects to the increase in CNI. NO decreases and PM decreases with lower bmep. Reduced injection pressure shows lower pHRR, widened HRR, retarded combustion phase. CNI decreases. Entire design factors change to lowering CNI. NO decreases and PM increases. Lower EGR ratio shows widened HRR, lower pHRR, advanced combustion phase. CNI decreases with lower EGR. Lower pHRR and wider HRR affects to the decrease in CNI. NO increases and PM decreases. Reduced swirl shows widened HRR and lower pHRR under the same combustion phase. CNI decreases with the wider HRR and lower pHRR. NO decreases and PM increases. Lastly, increase in pilot quantity shows widened HRR and lower pHRR under the same combustion phase. The results of pilot quantity were operated under the different total amount of fuel. It is difficult to use as combustion parameter for the optimization. CNI decreases with the higher pilot injection quantity. NO decreases and PM increases. These results show the effect of each combustion parameter on CNI although the design factors behave differently; some change towards the decrease in CNI, others change towards the increase in CNI.

According to the experimental results, noise reduction was achieved in view of exhaust gas emissions and bmep for the practical applications by the use of various combustion parameters, which are main injection timing, injection pressure, swirl in chamber and EGR ratio. As a result, CNI decreases by 3.6 dB with less loss of bmep and decrease in exhaust gas emissions. PM and NO emissions were slightly reduced by 0.302 FSN and 15.5 ppm respectively.

Reference

[1] Dieselnet, http://www.dieselnet.com/standards/eu/ld.php.

[2] Energy Efficiency and Renewable Energy Office of Transportation Technologies, "Homogeneous Charge Compression Ignition (HCCI) Technology: A Report to the U.S. Congress", U.S. Department of Energy, 2001.

[3] Bruno M, Spessert and Hans A. Kochanowski, Diesel Engine Noise Emission, Springer, Berlin Heidelberg, p 489-498, 2010.

[4] Gang Sheng, Vehicle Noise, Vibration and Sound Quality, SAE International, p 206, 2012

[5] Heywood, J. B., "Internal Combustion Engine Fundamentals", McGraw-Hill, 1988, ISBN 0-07-100499-8

[6] S. Kobori, T. Kamimoto, A. A. Aradi, "A study of ignition delay of diesel fuel sprays", International Journal of Engine Research February 1, 2000 vol. 1 no. 1 29-39

[7] Yu, T., Uyehara, O., Myers, P., Collins, R. et al., "Physical and Chemical Ignition Delay in an Operating Diesel Engine Using the Hot-Motored Technique," SAE Technical Paper 560061, 1956, doi:10.4271/560061.

[8] Ikegami, M., Shioji, M., and Kimoto, T., "Diesel Combustion and the Pollutant Formation as Viewed from Turbulent Mixing Concept," SAE Technical Paper 880425, 1988, doi:10.4271/880425.

[9] Edwards, C., Siebers, D., and Hoskin, D., "A Study of the Autoignition Process of a Diesel Spray via High Speed Visualization," SAE Technical Paper 920108, 1992, doi:10.4271/920108.

[10] Tadashi Murayama, "A Simulation of Diesel Engine Combustion Noise", SAE paper 760552, 1976

[11] Busch, S., Zha, K., Miles, P., Warey, A. et al., "Experimental and Numerical Investigations of Close-Coupled Pilot Injections to Reduce Combustion Noise in a Small-Bore Diesel Engine," SAE Int. J. Engines 8(2):2015, doi:10.4271/2015-01-0796.

[12] Vuilleumier, D., Selim, H., Dibble, R., and Sarathy, M., "Exploration of Heat Release in a Homogeneous Charge Compression Ignition Engine with Primary Reference Fuels," SAE Technical Paper 2013-01-2622, 2013, doi:10.4271/2013-01-2622.

[13] M. Badami, F. Mallamo, F. Millo and E. E. Rossi, "Influence of Multiple Injection Strategies on Emissions, Combustion Noise and BSFC of a DI Common Rail Diesel Engine", SAE Paper 2002-01-0503, 2002

[14] Yoshihiro Hotta, Minaji Inayoshi and Kiyomi Nakakita, "Achieving Lower Exhaust Emissions and Better Performance in an HSDI Diesel Engine with Multiple Injection", SAE paper 2005-01-0928, 2004

[15] Sylvain Mendez and Benoist Thirouard, "Using Multiple Injection Strategies in Diesel Combustion: Potential to Improve Emissions, Noise and Fuel Economy Trade-Off in Low CR Engines", SAE paer 2008-01-1329, 2008

[16] Fuyuto, T., Taki, M., Ueda, R., Hattori, Y. et al., “Noise and Emissions Reduction by Second Injection in Diesel PCCI Combustion with Split

Injection," SAE Int. J. Engines 7(4):1900-1910, 2014, doi:10.4271/2014-01-2676

[17] Shibata, G., Ishi, K., Ushijima, H., Shibaike, Y. et al., "Optimization of Heat Release Shape and the Connecting Rod Crank Radius Ratio for Low Engine Noise and High Thermal Efficiency of Premixed Diesel Engine Combustion," SAE Technical Paper 2015-01-0825, 2015, doi:10.4271/2015-01-0825.

[18] Gen Shibata, Yushi Shibaike, Hirooki Ushijima and Hideyuki Ogawa, "Identification of Factors Influencing Premixed Diesel Engine Noise and Mechanism of Noise Reduction by EGR and Supercharging", SAE Paper 2013-01-0313

[19] Hwang, Seon-Yang, et al., "Noise reduction and sound quality improvement of valve train in V6 gasoline engine." 2005-01-1834. SAE Technical Paper, 2005.

[20] Braun, Charles W., et al., "Acoustic Noise Assessment of Gasoline Direct Injection Fuel Injectors Using Taguchi Methods." 2011-01-1216. SAE Technical Paper, 2011.

[21] Watanabe, Atsushi, et al. "Noise Reduction in Gasoline DI Engines." 2011-01-0930. SAE Technical Paper, 2011.

[22] Tariq, Syed Mohammad, and Manas Tripathi., "Robust Engineering Methodology for Pulsation Noise Reduction in Gasoline Vehicles." 2013-01-2740. SAE Technical Paper, 2013.

[23] Zugo, S. Christopher, et al., "Acoustic Holography for High Pressure Fuel Injector Noise Measurements." 2014-01-1679. SAE Technical Paper, 2014.

[24] Lu, Ming-Hung, and Ming Une Jen., "Intake/Exhaust noise reduction with rig test optimization–case studies." 1999-01-1660. SAE Technical Paper, 1999.

[25] Sato, Naoki, and Yasuo Miura., "Study on exterior idling sound quality evaluation method for diesel engine trucks." 1999-01-1739. SAE Technical Paper, 1999.

[26] Terazawa, Noriyoshi, Yoshihiko Kozawa, and Tatsuo Shuku., "Objective evaluation of exciting engine sound in passenger compartment during acceleration." 2000-01-0177. SAE Technical Paper, 2000.

[27] Sasaki, Masaru, and Kazuhiro Nakashima., "Human auditory models and sound quality evaluation method for diesel noise." 2007-01-2219. SAE Technical Paper, 2007.

[28] Todd Tousignant, Thomas Wellmann and Kiran Govindswamy ,"Application of Combustion Sound Level (CSL) Analysis for Powertrain NVH Development and Benchmarking" SAE paper 2009-01-2168, 2009

[29] Shahlari, A., Hocking, C., Kurtz, E. and Ghandhi, J., "Comparison of Compression Ignition Engine Noise Metrics in Low-Temperature Combustion Regimes," SAE Int. J. Engines 6(1):2013, doi:10.4271/2013-01-1659.

[30] Jung, I., Jin, J., So, H., Nam, C. et al., "An Advanced Method for Developing Combustion Noise through the Analysis of Diesel Combustion," SAE Int. J. Engines 6(2):2013, doi:10.4271/2013-01-1901.

[31] Torregrosa AJ, Broatch A, Martín J, Monelletta L., "Combustion noise level assessment in direct injection Diesel engines by means of in-cylinder pressure components.", Meas Sci Technol 2007;18(7):2131e42.

[32] C. C. Shanjin Wang, Fabrice Gautier, "Optimization of Combustion Noise of Modern Diesel Engines for Passenger Cars," SAE, 2007,2007-01-2379.

[33] C. C. Shanjin Wang, Nicolas Duclaux, Marc Paquien, "Noise Optimization of Diesel Engines with New Combustion Systems," SAE, 2009,2009-01-2081.

[34] Li W, Gu F, Ball AD, Leung AYT, "A study of the noise from diesel engines using the independent component analysis", Mechanical Systems and Signal Processing 2001;15:1165-84.

[35] T. PRIEDE, "Problems and developments in automotive engine noise research" SAE paper 790205, 1979.

[36] Russell M F and Haworth R, "Combustion noise from high speed direct injection Diesel engines", SAE Paper 850973, 1985.

[37] Anderton D 1979, "Relation between combustion system and noise", SAE Paper 790270, 1979.

[38] AUSTEN, A. and PRIEDE, T., "ORIGINS OF DIESEL ENGINE NOISE," SAE Technical Paper 590127, 1959, doi:10.4271/590127.

[39] Hayes, C. D., Lamers, M. D., "Octave and One-third Octave Acoustic Noise Spectrum Analysis", NASA Technical Report 19670006729, 1967.

[40] Asad, Usman, and Ming Zheng. "Fast heat release characterization of a diesel engine." International Journal of Thermal Sciences 47.12 (2008): 1688-1700.

[41] R.B. Krieger, G.L. Borman, The computation of apparent heat release for internal combustion engines, in: Proc. Diesel Gas Power, ASME 66-WA/DGP-4, 1966.

[42] J.A. Gatowski, E.N. Balles, K.M. Chun, F.E. Nelson, J.A. Ekchian, J.B. Heywood, "Heat release analysis of engine pressure data", SAE 841359.

[43] M.F.J. Brunt, H. Rai, A.L. Emtage, "The calculation of heat release energy from engine cylinder pressure data", SAE 981052.

[44] M.F.J. Brunt, K.C. Platts, "Calculation of heat release in direct injection diesel engines", SAE 1999-01-0187.

[45] Nuszkowski, J., and G. J. Thompson. "Application and repeatability of transient heat release analysis for heavy diesel engine." SAE paper (2009): 01-1125.

초 록

최근 디젤엔진의 기술 진보는 무공해, 고출력 및 사용자 편의성의 세 가지 기조로 이루어지고 있다. SI 엔진과 비교하였을 때, 디젤 엔진은 고압축비로 인한 연소 특성을 원인으로 하는 문제점을 가지고 있다. 소음과 진동은 널리 알려진 주요한 디젤 엔진의 당면 해결과제로, 운전자 편의성의 측면에서 연구가 활발히 진행되고 있다.

본 연구에서는 엔진 내부의 열발생률을 모사하여 연소의 형상이 연소음에 미치는 영향에 대해 다루었다. 기존의 소음 저감을 위한 접근 방식은 다양한 연소조건들을 변화시켜가면서 이에 대한 소음수준을 측정하여 연소인자들을 최적화 하는 방식이다. 이번 연구에서 제시한 방법론은 기존 방식과는 반대로, 연소의 결과로 발생된 열발생률의 형상이 소음에 미치는 영향을 분석하고자 하였다.

모사된 열발생률을 통해 계산된 압력곡선으로 연소음지수(CNI)를 구할 수 있으며, 그 결과 최대 열발생률, 열발생률의 폭 그리고 연소상의 세 가지 설계인자를 도출하였다. 그 결과로, 최대 열발생률이 낮아질수록, 열발생률의 폭이 클수록, 연소상은 지각될수록 CNI 값은 감소한 것을 확인할 수 있었다.

다음으로, 위의 과정을 통해 제시된 설계 인자의 적용 가능성 확인을 위해 실험을 통하여 설계 인자들에 영향을 주는 엔진 운전 변수들을 선정하였다. 선정된 운전 변수들의 수준을 변화시켜가며 이에 대한 설계 인자들의 변화와 배기배출물 수준의 변화를 확인하였다. 연료 분사시기, 분사압력, EGR, Swirl 및 Pilot 연료량의 다섯 가지 운전 변수들을 선정하였다.

마지막으로, 초기 운전조건에서부터 선정된 인자들을 변화시켜가며 배기배출물과 bmep 수준을 유지한 상태에서 CNI 값을 3.6 dB 가량 낮추었다. 실험은 배기배출물 및 출력을 고려한 가운데서 초기 조건에서 연소인자들을 변화시켜가며 설계 인자들의 변화가 CNI 값을 낮추는

운전점을 탐색하는 방식으로 진행되었다. 최종적으로 얻어진 결과는 분사시기 지각 및 Swirl 감소, 분사압 감소, EGR ratio 감소의 3 가지 단계로 분류하였다.

주요어 : 열발생률, 열발생률 설계, 연소음지수(CNI), 연소음, 디젤 엔진, 소음 저감

학번 : 2013-23081